Theor Chem Acc (2000) 103:451–462
DOI 10.1007/s002149900075

Theoretical
Chemistry Accounts

Regular article

Hydride-transfer transition structure as a possible unifying redox step for decscribing the branched mechanism of glutathione reductase. Molecular-electronic antecedents

F. Iribarne[1], **M. Paulino**[1], **O. Tapia**[2]

[1] Cátedra de Química Cuántica, Facultad de Química, Universidad de la República, Gral. Flores 2124, 11800, Montevideo, Uruguay
[2] Department of Physical Chemistry, Uppsala University, P.O. Box 532, S-751 21, Uppsala, Sweden

Received: 23 November 1998 / Accepted: 22 June 1999 / Published online: 4 October 1999

Abstract. For glutathione reductase (GR), a mammalian reduced nicotinamide adenine dinucleotide phosphate dependent flavoenzyme participating in free-radical detoxification pathways, we present a quantum chemical study addressing aspects of its electronic mechanism. The system is known to sustain both ping-pong and sequentially ordered mechanisms depending upon particular conditions. Isoalloxazine and nicotinamide-N-protonated rings are taken as a minimum model. The AM1 method and the AMSOL program are used throughout. Starting from a transition-state structure, docked at GRs active site, and successively including molecular elements of the active site relevant to the redox processes, geometry-optimized binary and tertiary complexes are characterized suggesting a plausible description for the sequentially ordered mechanism. The ping-pong mechanism relates to an electron-transfer (ET) mechanism. An ET binary complex between nicotinamide and the isoalloxazine ring was characterized. Its electronic structure is controlled by the protonation state of the proton relay found at this active site. The excess proton in the relay comes from the previous hydride-transfer step. The experimental stereoselectivity is then fulfilled. The state of charge (standard Mulliken population analysis) shows an excess of two electrons on the isoalloxazine ring and almost one on the nicotinamide ring. The overall results suggest that both mechanisms can be controlled by the same hydride-transfer structure, the difference between them being determined by changes in the oxidized coenzyme binding strength to the protein and/or the strength of the protein–substrate interactions.

Key words: Branched mechanism – Glutathione reductase – Catalytic mechanism – Transposed hydride transfer – Proton relays

Correspondence to: O. Tapia

1 Introduction

Glutathione reductase (GR) catalyzes the reduction of oxidized glutathione disulfide (GSSG) via a widely accepted electron-transfer (ET) mechanism. Electrons are moved from the nicotinamide adenine dinucleotide phosphate (NADPH) towards the substrate by using the flavine adenine dinucleotide (FAD) as pictorially described in Fig. 1. Under physiological conditions, the system exhibits a ping-pong mechanism [1], where two redox events are well separated in time:

1. NADPH oxidation leading to a reduced enzyme, with the $NADP^+$ leaving the enzyme (ping).
2. The pong step corresponds to substrate binding into the reduced enzyme and final reduction to two GSH (glutathione) molecules. The isoalloxazine ring of FAD and possibly the redox-active disulfide (SS) bridge act as a two-electron acceptor [1, 2]. As a catalyst, GR has some peculiarities. As shown by Mannervik [3] and Williams [4], GR presents a complex mechanistic scheme. Besides the ping-pong, they found a sequentially ordered (SO) mechanism when some special substrates are used. In fact, the system has a branched mechanism, reflecting a competition between these alternatives, namely, ping-pong and SO mechanisms. Bearing in mind that for some specific mutation the mechanism of GR changes from ping-pong to SO [5], it is clear that both paths are accessible for the enzyme.

From a mechanistic viewpoint, the SO mechanism can be related to hydride-transfer (HT) reactions. A quantum chemical transition structure (TS) was determined by Diaz et al. [6] using the isoalloxazine/nicotinamide molecular model. As this (TS) can be accommodated at the active site of GR without steric hindrances, these authors suggested that the SO mechanism could be related to the HT mechanism, an idea backed by previous experimental evidence [1, 7]. There is, however, one unknown factor concerning the fate of the proton because it is acknowl-

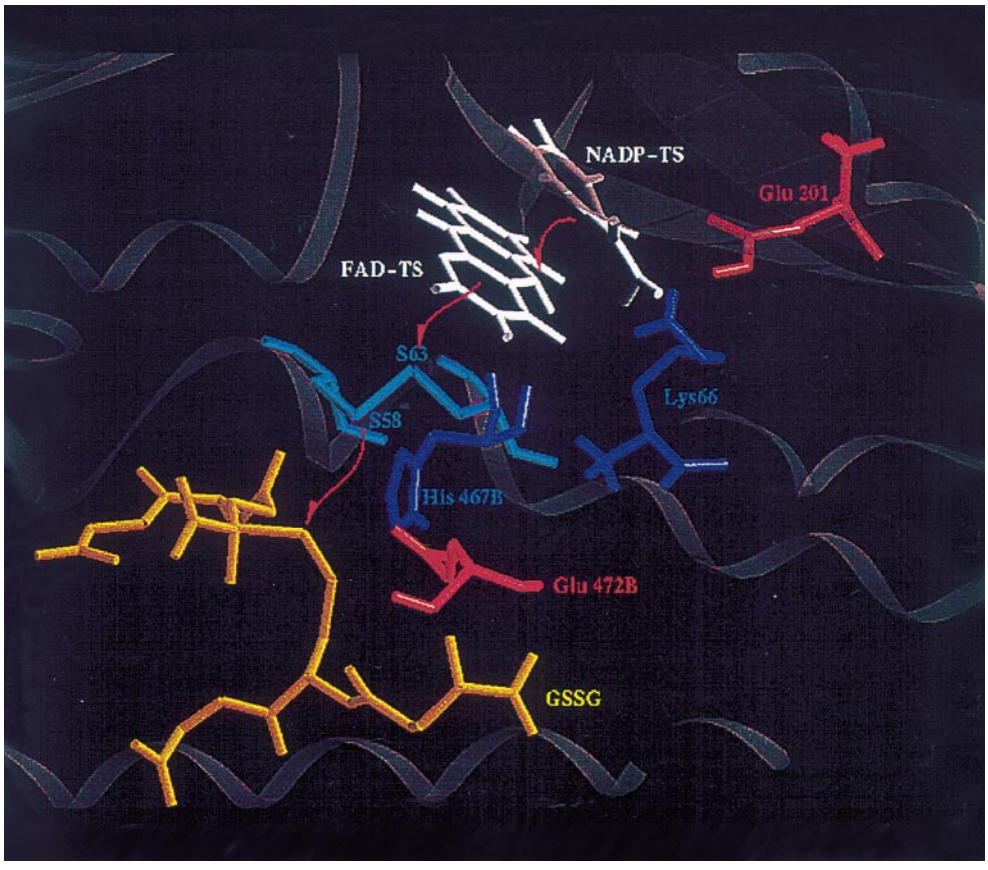

Fig. 1. Flavine adenine dinucleotide–nicotinamide adenine dinucleotide phosphate transition structure (*FAD-NADP-TS*) docked at the binding site of glutathione reductase (*GR*). Participants in the overall enzymatic transfer reaction are drawn as *colored sticks*: *white*, FAD-NADP-TS model; *cyan*, enzymatic disulfide bridge (Cys58-Cys63); *blue*, Lys66 and His467B; *red*, Glu201 and Glu 472B; *yellow*, glutathione substrate. The secondary structure of GR is shown as a *background ribbon* model

edged that there is no direct transfer of a hydride ion from the NADPH to the substrate GSSG. It was suggested then that residues Lys66 and Glu201 (numbering from the human erythrocyte sequence) may act as a proton relay to help a transposed HT in the N-site (NADP active site where the nicotinamide ring faces the isoalloxazine ring). In this manner, for the global interconversion, the hydrogen transferred from the C_4 center in NADPH will stay around the N-site trapped by this proton relay system and will later be released to the surrounding media. The substrate, GSSG is reduced by accepting two electrons via its interaction with the redox-active SS bridge located at the G-site (GSSG binding site, see Fig. 1). The proton required to make the hydride is picked up from the G-site. This is the reason why the mechanism is called a transposed HT. A fundamental difference between the SO mechanism and the ping-pong path appears to be the presence of stable binary $NADP^+$-FAD-SS and tertiary $NADP^+$-FAD-SS-GSSG complexes in the SO pathway. The two electrons and one proton are then located somehow at the FAD-SS and the proton relay system.

From a theoretical viewpoint, besides the TS for HT by Diaz et al. [6], very little is known about these mechanisms. The fate of the proton at the N-site is equally important in both mechanisms. One may conjecture that the C_4 hydrogen interacting with Glu201 may be transferred to this side chain and so the ET and the HT may have alternative pathways, thereby explaining the presence of both channels [8]. This simple explanation is not supported by experimental evidence because the hydrogen transferred from C_4 in NADPH fulfills a stereoselectivity constraint. There is ample evidence indicating that the hydrogen exchanged corresponds to the one facing the FAD ring [9–12]; therefore, both mechanisms must follow the same pathway in so far as hydrogen transfer is concerned. The main assumption here is that the TS for HT is common to both mechanisms.

To document whether a theoretical difference could be established between the SO and the ping-pong mechanisms, we studied the former with the aim of establishing the possible presence of stable species representing the binary and tertiary complexes. No attempt was made to calculate rates. The starting geometry is the TS and the N-site proton shuttle, whose position was retrieved from the X-ray structure. At a later stage, the redox-active SS groups and the GSSG in the G-site were included. The mapping was performed from the perspective of the activated complex formed by isoalloxazine and nicotinamide rings. From that saddle point the system was allowed to relax towards different complexes whose energies and structures were determined with the help of geometry-optimization procedures. A number of AM1 quantum chemical semiempirical calculations [13] were performed on these molecular systems. The results show that complexes fulfilling the requirement for substrate reduction can be found if, in a final stage, a proton coming from the proton relay found at the G-site is added to the system.

The documentation of a possible SO mechanism does not prove that the ET would follow a path with the same TS. This point was further investigated by searching for geometric configurations displaying the signature of ET,

namely, two electrons on the isoalloxazine ring and a positive charge at the oxidized nicotinamide ring. Such structures were found below the energy threshold for the TS and, interestingly, above the energy of the corresponding binary complexes. The role of the proton relay structure is emphasized in these calculations. The overall results reported here strongly suggest that both mechanisms can be related to the same TS, the difference being controlled by factors such as geometric relaxation rates and coenzyme binding strength, which are indirectly related to the redox step.

2 System, models and methods

2.1 System

GR is a mammalian NADPH-dependent flavoenzyme taking part in free-radical detoxification processes [2, 14, 15]. It catalyzes the reduction of GSSG yielding two reduced GSH molecules. GSH is the major thiol metabolite in mammalian cells helping counteract the attacks exerted by reduced oxygen derivatives such as the superoxide anion, hydrogen peroxide and the hydroxyl radical [16].

The catalytic mechanism of GR was addressed early in experimental work by Mannervik and coworkers [3, 17–20] on the reduction of 2,4,6-trinitrobenzene sulfonate with NADPH. It was shown there that the reaction mechanism has a branched nature, with one loop proceeding via a ping-pong mechanism and a second loop corresponding to a SO mechanism and with each member of the molecular ensemble taking one of the two paths although they share the NADPH binding step. The ping-pong case corresponds to two redox steps separated in time and space as mentioned previously. For the SO mechanism, it is required that an enzyme–$NADP^+$ complex is formed first, followed by subsequent production of the tertiary complex: substrate-enzyme–$NADP^+$ [3, 6].

The ping-pong pattern applies to the reduction of the natural substrate GSSG [1, 21]. Here, NADPH effectively leaves two electrons and one proton yielding a reduced enzyme (E-$FADH_2$). It is this species which binds GSSG and reduces it to two GSH molecules. The coexistence of both loops can be inferred from experiments by Berry et al. [5] with the mutated enzyme of *Escherichia coli* at Tyr177 (Tyr197 in the human enzyme). The Tyr177Gly mutated enzyme changes the mechanism from ping-pong to SO, and a concomitant loss of activity is verified when this tyrosine is replaced by either serine or glycine. Such results show that both pathways are accessible to the catalytic machinery provided by the protein structure (and solvent).

2.2 Model

In the theoretical analysis of Diaz et al., the transit via the SO mechanism implies the population of the TS for HT. The protonation states of Lys66 and Glu201 would be the factors controlling the possible transfer of the hydride, and will take the form of a proton transfer from the TS-like (successor complex) to the N-site. It is commonly accepted that there is no HT to the G-site. The present work conforms with this postulate.

The approach used here consists of exploring the energy hypersurface to find out whether intermediate complexes are accessible and stable to atomic fluctuations (geometrically minimized structures). Once the HT TS states are populated, particular paths producing a given mechanism may depend upon the formation of specific intermediates in an energy downhill process.

A search for binary and tertiary complexes was attempted by exploring the AM1 hypersurface in vacuo, in the neighborhood of the molecular system built with the previously mentioned TS structure and including Lys66 and Glu201. The models representing the active site of GR were constructed from the coordinates obtained from the Brookhaven Protein Data Bank [22]. The peptide groups were capped so that they were represented by the zwitterion forms. These atoms may be kept fixed, while the side-chain atoms can be fully geometry-optimized. To test the relative energy differences to solvent polarization effects, calculations were carried out with AMSOL [23].

The isoalloxazine molecule represents the redox-active part of FAD. The redox head of NADPH is represented by 1,4-dihydro-3-amide pyridine (the nicotinamide residue). The geometry of the TS calculated by Diaz et al. [6] was used to seed the calculations.

2.3 Methods

Manipulations with coordinates at the active site were carried out with the program mdFRODO [24, 25]. The quantum calculations were performed with AM1 [13] by means of the AMSOL3.0 program. The AM1–SM2 model was used for polarization studies [23].

The geometry-optimized structures were checked with the PM3 semiempirical Hamiltonian [26], yielding results similar to those reported here with AM1. The TS geometry was obtained using ab initio calculations. Concerning geometries, these methods yield comparable results and so the models used here are fairly good representations of what one might expect when using other levels of theory [27–29].

2.4 Geometric configurations

A selection of the geometric parameters defining the most significant configurations explored in this work is given in Tables 1 and 2. Table 1 refers to the binary complexes case. Labeled models are taken as seeds for further studies leading to the tertiary complexes summarized in Table 2.

2.5 Proton affinity checking calculations

Given the fact that the models compared here mainly differ in the proton state of the relay couple, a validation of the AM1 calculation method was carried out. In effect, the proton affinities of some model systems were

Table 1. Geometric parameters found after exploring the energy hypersurface of the binary complex flavine adenine dinucleotide–nicotinamide adenine dinucleotide phosphate (*FAD-NADP*) models. Values corresponding to two different calculation levels (*1* = 1SCF, *2* = side-chain optimization). N_5 = isoalloxazine (Iso) acceptor, C_4 = nicotinamide donor, H_t = transferred proton, N_z = amine 66 nitrogen, O_{201} = carboxylate 201 oxygen, $H_{66'}$ = amine 66 proton, H_{201} = carboxylate 201 proton. Distances in angstrom. A series of structures selected for further study is indicated in *bold text*

Models	Optimization level	N_5-H_t	N_z-H_t	C_4-H_t	N_5-N_z	N_z-O_{201}	$H_{66'}$-O_{201}	N_z-H_{201}
Case 1								
$IsoH^-$.N**ADP**$^+$.$Lys66^+$.$Glu201^-$	1 (**1A1**)	1.00	2.11	2.16	3.10	2.15	2.00	
$IsoH^-$.N**ADP**$^+$.$Lys66^+$.$Glu201^-$	2 (**1A2**)	1.05	3.36	1.69	4.09	2.73	1.95	
$IsoH^-$.N**ADP**$^+$.$Lys66^+$.$Glu201^-$	3	1.01	3.45	3.25	4.36	2.73	1.95	
Case 2								
$IsoH^-$.N**ADP**$^+$.$Lys66^+$.$Glu201^-$	1	1.50	1.60	2.21	3.10	2.15	1.26	
$IsoH^-$.N**ADP**$^+$.Lys66.Glu201	2	1.01	4.01	3.38	4.54	3.73	0.97	
$IsoH^-$.N**ADP**$^+$.Lys66.Glu201	3	1.01	3.91	2.93	4.49	3.73	0.97	
Case 3								
$IsoH^-$.N**ADP**$^+$.$Lys66^+$.$Glu201^-$	1	1.20	1.93	2.02	3.10	2.15	1.48	
$IsoH^-$.N**ADP**$^+$.$Lys66^+$.$Glu201^-$	2	1.05	3.38	1.69	4.10	3.73	1.96	
$IsoH^-$.N**ADP**$^+$.$Lys66^+$.$Glu201^-$	3	1.01	2.85	2.29	3.55	3.73	1.96	
Case 1								
Iso^-.N**ADP**$^+$.$Lys66^+$.Glu201	1 (**1B**)	1.23	0.99	2.14	2.11	3.14		4.31
$IsoH^-$.N**ADP**$^+$.Lys66.Glu201	2 (**1C**)	1.01	3.26	3.06	3.87	3.00		2.51
$IsoH^-$.N**ADP**$^+$.Lys66.Glu201	3	1.01	3.23	3.02	3.89	3.00		2.51
Case 2								
Iso^-.N**ADP**$^+$.$Lys66^+$.Glu201	1	1.08	1.08	2.21	2.11	3.14		2.51
$IsoH^-$.N**ADP**$^+$.Lys66.Glu201	2	1.01	3.51	3.06	4.18	3.06		2.50
$IsoH^-$.N**ADP**$^+$.Lys66.Glu201	3	1.01	3.58	3.17	4.25	3.06		2.50
Case 3								
Iso^-.N**ADP**$^+$.$Lys66^+$.Glu201	1	0.95	1.18	2.32	2.11	3.14		2.29
$IsoH^-$.N**ADP**$^+$.Lys66.Glu201	2	1.01	3.38	3.06	4.00	3.00		2.55
$IsoH^-$.N**ADP**$^+$.Lys66.Glu201	3	1.01	3.38	3.03	4.05	3.00		2.53

calculated and the AM1 results compared with experimental data. The theoretical and experimental values for the models tested are listed in Table 3. It is evident that the calculations systematically underestimate the proton affinities of bases as well as of acids (relative errors ranging from 13 to 25%). Consider now the standard reaction scheme $RCOO^- + NH_3^+ \rightarrow RCOOH + NH_2$. For butyric acid and butylamine in Table 3, the calculated ΔH (AM1) and experimental protein affinity values are −134 and −130 kcal/mol, respectively. The resulting relative error of the AM1 method is roughly 3%.

The pairs, 1A2-1C (Table 1, Fig. 2) and 2A2-2C (tertiary models of Table 2) represent supermolecules in which the hydrogen-bonding pair (Lys66–Glu201) is in an environment containing relevant local features of the active site. In this context, the above reaction accounts for the overall transformation of going from 1A2 to 1C and from 2A2 to 2C. The energy difference favors 1C above 1A2 and 2C above 2A2 (−14.4 and −19.2 kcal/mol, respectively). The energy differences are significant in view of the small error found with respect to experiments.

3 Results

3.1 N-site models

First, we focus attention on the stability of the transferred hydrogen in the TS towards interactions with the Lys66–Glu201 dyad. The geometry results summarized in Tables 1 and 2 illustrate the extent to which the search was carried out. The effective charges are given for the relevant structures in Figs. 2–4. Among the structures reported, some of them were geometry-optimized from the TS. This means the isoalloxazine ring has a butterfly conformation so that its hydride acceptor center (N_5) has the hybridization state prepared to form a N_5-H bond.

The distance between N_5 of the hydride receptor center of isoalloxazine and N_z of Lys66 was changed to define configurations 1A1 and 1B (Table 1), and 2A1 and 2B (Table 2) where the redox-active SS bridge and model substrate are included in the calculations. The main-chain atoms of Lys66 and Glu201 (represented with a grey star in Figs. 2–5) were kept fixed together with the atoms in isoalloxazine and nicotinamide. The side chains were first geometry-optimized followed by an internal geometry optimization of the isoalloxazine ring for all hydrogen distributions selected here (not shown).

The most relevant binary complexes are depicted in Fig. 2. The initial configuration 1A1 was chosen as a successor complex where the transferred hydrogen (H_t) is set near N_5. The side-chain optimization (1A2) brings this hydrogen towards the N_5–C_4 axis in a position reminiscent of the HT path. This can be seen in Table 1 where the C_4-H_t distance is about 1.7 Å instead of the 2.2 Å in 1A1.

Table 2. Geometric parameters found after exploring the energy hypersurface of the tertiary complex FAD-NADP-substrate models. Values corresponding to two different calculation levels (*1* = SCF, *2* = side-chain optimization). Atom names as in Table 1, S_{58} = Cys58 sulfur, S_{63} = Cys63 sulfur, S_I = oxidized glutathione (*GSSG*) CysI sulfur, S_{II} = GSSG CysII sulfur. Distances in angstrom

Models	Optimization level	N_5-H_t	N_z-H_t	C_4-H_t	N_5-N_z	N_z-O_{201}	H_{66}-O_{201}	N_z-H_{201}	S_{63}-N_5	S_{63}-N_z	S_I-N_5	S_I-N_z
$IsoH^-.NADP^+.Lys66^+.Glu201.Cys58.Cys63.GSSG$	1 (2A1)	1.01	3.26	3.06	3.87	3.00	2.55		4.18	7.19	10.1	11.8
$IsoH^-.NADP^+.Lys66^+.Glu201.Cys58.Cys63.GSSG$	2 (2A2)	1.01	3.73	3.11	4.35	2.77	1.96		4.18	7.33	10.1	11.8
$IsoH^-.NADP^+.Lys66.Glu201.Cys58.Cys63.GSSG$ dist. N_5-N_z = 2.58 Å	1	1.01	1.90	3.06	2.58	4.06		3.37	4.18	5.91	10.1	10.9
$IsoH^-.NADP^+.Lys66.Glu201.Cys58.Cys63.GSSG$	2	1.01	2.83	3.09	3.47	3.14		2.51	4.18	6.61	10.1	11.4
$Iso^-.NADP^+.Lys66^+.Glu201.Cys58.Cys63.GSSG$	1 (2B)	1.35	0.97	2.80	2.18	3.92		3.26	4.18	5.53	10.1	10.6
$IsoH^-.NADP^+.Lys66.Glu201.Cys58.Cys63.GSSG$	2 (2C)	1.01	2.44	2.99	3.24	3.13		2.80	4.18	6.33	10.1	10.7
$Iso^-.NADP^+.Lys66^+.Glu201.Cys58.Cys63.GSSG$ dist. N_5-N_z = 2.58 Å	1	2.44	0.99	2.67	2.58	3.71	3.13	2.91	4.18	5.91	10.1	10.9
$Iso^-.NADP^+.Lys66^+.Glu201.Cys58.Cys63.GSSG$	2 (2B2)	2.56	0.99	2.45	2.90	5.00	4.08	4.55	5.53	6.73	10.5	11.2

Table 3. Numerical test comparison of proton affinities (*PA*) calculated using the AM1 method and experimental results. The calculated ΔH for the reaction: $XH \rightarrow X + H^+$ is assumed to represent the proton affinity of X (X: either acid or base). The experimental PAs are according to Kebarle P (1977) Annu Rev Phys Chem 28: 445

Compound	(kcal/mol)		
	$-E$	$-\Delta H$	PA
n-Butyric acid	29138	298	346
n-Butyrate	28840		
Piridine	21270	162	218
Piridinium	21108		
n-Butylamine	20099	164	216
n-Butylammonium	20263		

The structure 1B describes protonated Glu201 and another proton shared by N_5 and N_z. This situation would be obtained if the ion-pair between Lys66–Glu201 first reverted to a neutral hydrogen-bonded complex so that Lys66 might act as a proton acceptor in face of the N_5-H hydrogen-bonding donor. Very little charge transfer (0.11) from NADP obtains.

The geometry optimization of 1B leads to structure 1C. The hydrogen stays at N_5 and a neutral hydrogen-bonded complex remains between Lys66 and GluH201. An increased charge transfer (0.78) from NADP can be seen from the figure labels.

Instead of starting the optimization from 1B, if one moves Lys66 away, the proton at N_5 follows N_z and one gets the structure 1B2. This structure has a strong interaction between the amide and GluH201; it corresponds to a dead end in so far as ET is concerned because one would expect a full negative charge on FAD (close to −2) and a full positive charge on NADP (close to +1), but, as shown in the figure, such is not the case.

On optimizing the ring structures of 1A2 and 1C (data not shown) the charge transfer from NADP increases (+0.98), while the optimized isoalloxazine ring attains a charge of −0.98. These structures are related to the HT mechanism. They qualify as a stable intermediate complex corresponding to the isoalloxazine ring protonated at N_5. For both structures, N_5 is protonated although the direction of the N_5-H bond with respect to the N_5–C_4 axis has changed. Their side-chain optimized structures have energies of −200714 kcal/mol and −200728 kcal/mol, respectively, showing the neutral pair to be more stable than the ion-pair form.

The remaining optimized structure shown in Fig. 2 is 1B2, with an energy of −200749 kcal/mol. As stated before, this structure seems to be an abortive complex in the sense that there is no charge separation between FAD and NAD.

The charge partitioning shows a marked difference between the hydride complex (1A2 and 1C in Fig. 2) and the charge-transfer complex (1B2 in Fig. 2). In the first case, there is an extended charge shift among all constituents at the N-site (1A2 and also in the fully ring optimized structure) which would produce charge-transfer interactions. In the 1C case the electrons are also located in the FAD ring while a proton is to be found in the

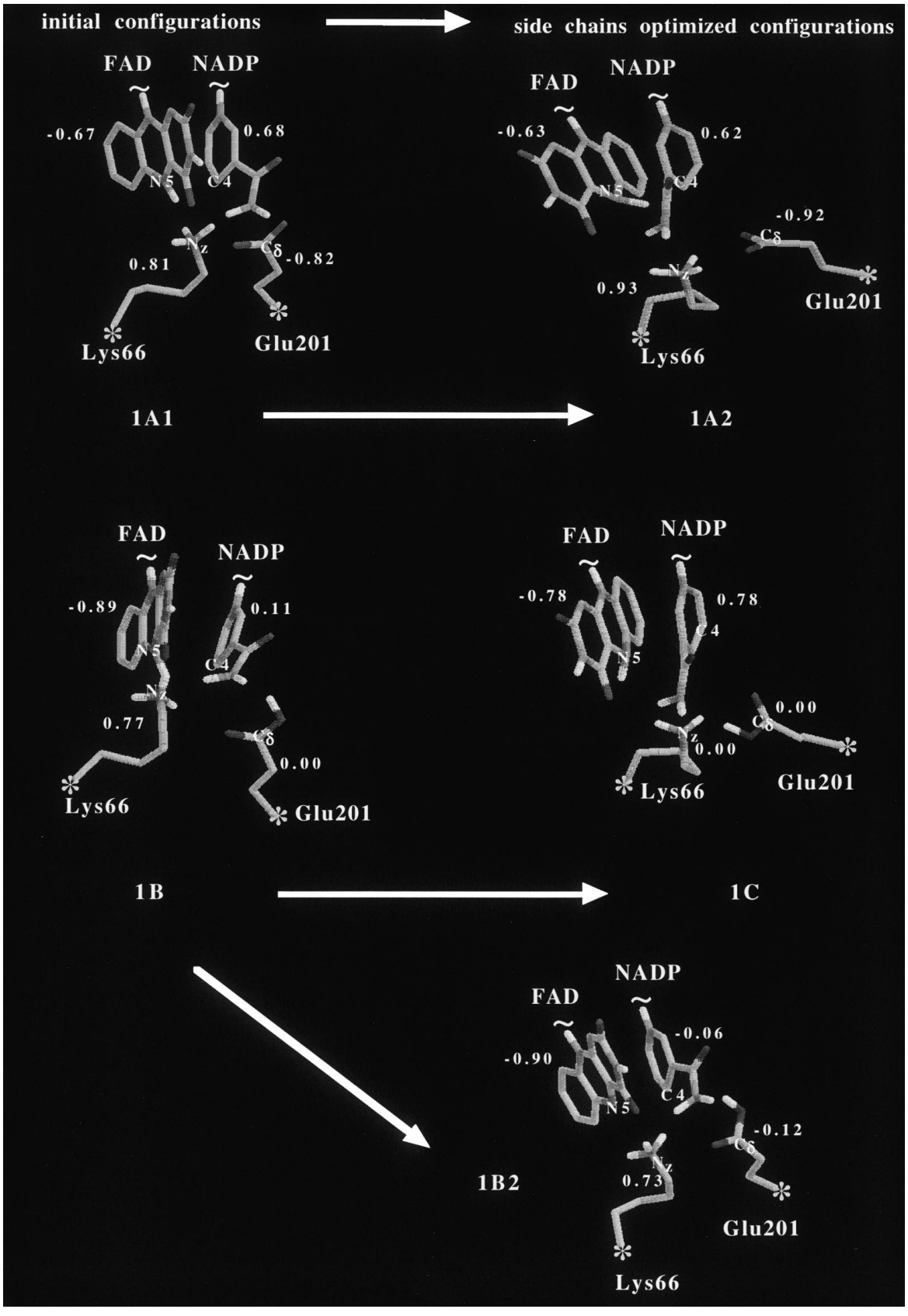
initial configurations
side chains optimized configurations
FAD
NADP
-0.67
0.68
N5
C4
Nz
Cδ
0.81
-0.82
Lys66
Glu201
-0.63
0.62
-0.92
0.93
1A1
1A2
-0.89
0.11
0.77
0.00
-0.78
0.78
-0.06
-0.90
-0.12
0.73
1B
1C
1B2

◀

Fig. 2. Binary models. *1A1* ($E = -200524$ kcal/mol) and *1A2* ($E = -200714$ kcal/mol) are self-consistent-field (*SCF*) and side-chain optimization calculations of model isoalloxazine (*IsoH*$^-$). *NADP*$^+$.Lys66$^+$.Glu201$^-$, respectively. *1B* ($E = -200570$ kcal/mol) and *1C* ($E = -200728$ kcal/mol) are 1SCF and side-chain optimization calculations of model Iso$^-$.NADP$^+$.Lys66$^+$.Glu201 case 1 (initial distance between Iso atom N_5 and amine 66 atom N_z set at 2.18 Å), respectively. *1B2* ($E = -200749$ kcal/mol) corresponds to the side-chain optimization calculation of model Iso$^-$.NADP$^+$.Lys66$^+$.Glu201 case 2 (initial distance between Iso atom N_5 and amine 66 atom N_z set at 2.58 Å). "~" over Iso and nicotinamide rings indicates the point of linkage with the rest of the FAD and NADP molecules, respectively. "*" represents the Cα atoms of Lys66 and Glu201 which were kept fixed during side-chain optimization as well as the remaining main-chain atoms of residues (not included in the figure). *Numbers* near each group correspond to effective charge values

neutral Lys66–Glu201 forming a hydrogen-bonded complex, whereas in 1B2 all the charge concentrates in the isoalloxazine ring and in the Lys66 side chain.

One may argue that the redox-active SS bridge of the enzyme may play a role here. The results (not reported) show that models extended with the enzyme-active SS present a behavior similar to the simple binary arrangement.

The tertiary complexes were obtained by adding the GSSG, CH3-S-S-CH3, at the G-site as indicated in Fig. 3. As the situation of most interest here is the fate of the transferred hydrogen and the formation of a charge-transfer complex, we present results obtained from the initial configuration 2B.

The space disposition and effective charges are reported in Fig. 3. As was found for the binary complex, the N_5-N_z distance controls the fate of the hydride in this model study. If this distance is larger than 2.5 Å, structure 2B2, the N_5 proton leaves the isoalloxazine but a retro charge-transfer occurs towards NADP (−0.1). So the electrons are tied up to the full complex including the substrate.

For structure 2C, the hydride stays at the isoalloxazine ring. Very small charge transfer towards the substrate is detected here.

3.2 G-site expanded models

The possible role of the putative relay couple at the G-site (His467B and Glu472B) in the ensuing steps of the catalytic mechanism was tested. Some modifications were performed on the enzyme SS bridge of the extended models. In effect, in the models tested, a proton was first attached to the sulfur atom of Cys58 while both sulfurs comprising the enzyme SS bridge (S_{58} and S_{63}) were set apart to a final distance of 3 Å. As a result, the side chain moved so the bare S_{63} approached atom C_{4A} in isoalloxazine (distance of 3.3–3.4 Å). Massey et al. [2] have suggested this situation to be responsible for charge transfer. At this stage, the electrons are thought to be transferred from FAD to the enzyme SS bridge sitting at S_{58} since S_{63} is involved in a charge complex with the isoalloxazine ring. Hence, the breaking of the SS bridge is modeled here by protonating S_{58}.

After optimization of S_{58} and S_{63}, the atom charges (Fig. 4) show a charge transfer between C_{4A} and S_{63}, taking place only in the situation where the isoalloxazine ring is deprotonated (selected model 3B2, $E = -234455$ kcal/mol). In this case, the distance S_{58}-S_{63} is increased to 4.0 Å; the now negatively charged S_{63} is even closer to atom C_{4A} (2.8 Å). At the same time, the negative charge of the deprotonated flavine is considerably reduced. (Fig. 4). None of these changes are produced when the isoalloxazine ring is initially protonated (3C in Fig. 4, $E = -234474$ kcal/mol). Now, the system has a more stable configuration, i.e., the reunion of the sulfur atoms with the negative charge concentrated at the isoalloxazine ring. If charge transfer from the N-site to the G-site is sought, these results show that the isoalloxazine ring must first be deprotonated. This is not much of a surprise: the interesting new information is the proton-sink role of the Lys66-Glu201 side chains during such a process.

A series of AM1–SM2 [23] calculations were run aiming at sensing the effect of polarization in the relative stabilities of the various set-ups sketched in Figs. 2–4. A polarization effect is present in a protein environment. Since the solvation model corresponds to water, the results are used here to check the sensitivity of the energy gaps. The results (not presented here) essentially bolster the previous in vacuo findings as far as relative energies are concerned. For instance, the energy difference between 1C and 1A2 is virtually the same in vacuo and in AM1–SM2 surroundings.

3.3 ET configurations

In the proton-shuttle framework studied here, an ET configuration can be prompted if both Lys66 and Glu201 are protonated. A number of geometric set-ups were explored. Six significant structures are shown in Fig. 5. The parameter used to report changes is the N_5–C_4 distance. For the TS this distance is rather short (2.6 Å), while for the HT successor complex it is found in the range of 3.5 Å. In the scenario associated with the ET mechanism, the oxidized head of NADP must leave the N-site. We have checked the effect of such displacement by using distances of 3.0, 3.4 and 3.5 Å.

The results in Fig. 5 show the seed of an ET structure: about −1.8 *e* on the isoalloxazine ring and +0.8 *e* at the nicotinamide ring at 3.0 Å. A strong interaction between the side chains is apparent from the effective charges. Full ring optimization with fixed side chains at 3.5 Å suggests that the nicotinamide ring gains positive charge or retains its fully charged state. Note that there are not important variations if the nicotinamide ring is fixed at the junction with the rest of the coenzyme, or if it is allowed to move freely (Fig. 5).

One would like to compare the HT and ET models as regards their relative stability. This can be accomplished by energy-optimization calculations entailing the whole model configuration for each particular case (data not shown). For instance, the internal energy for the ET optimized structure at 3.0 Å is −200744 kcal/mol which is above the fully optimized 1A2 ($E = -200777$ kcal/

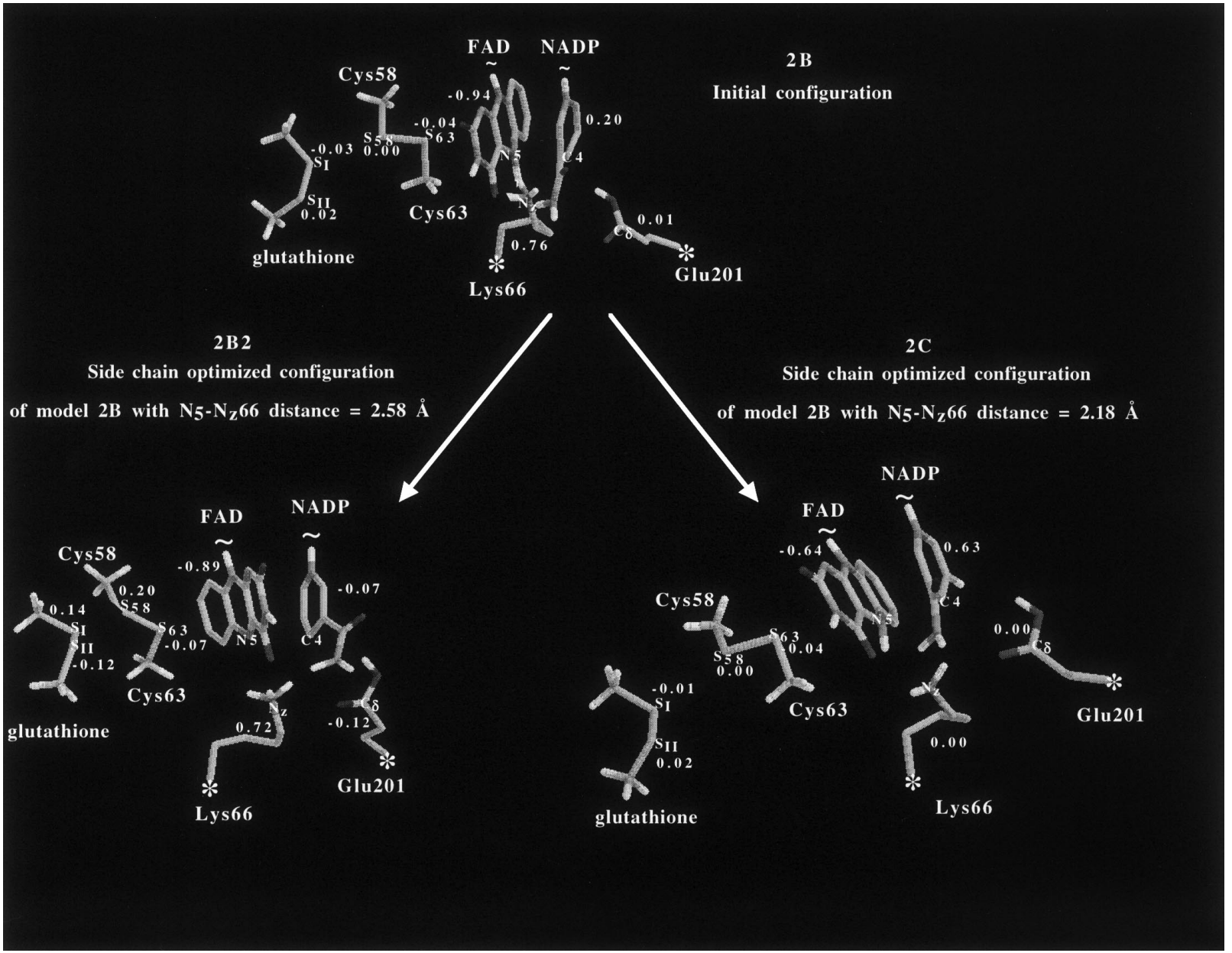

Fig. 3. Tertiary models. *2B* ($E = -233722$ kcal/mol) and *2C* ($E = -234334$ kcal/mol) are SCF and side-chain optimization calculations of model $Iso^{-}.NADP^{+}.Lys66^{+}$.Glu201.Cys58. Cys63. oxidized glutathione(*GSSG*) case 1 (initial distance between Iso atom N_5 and amine 66 atom N_z set at 2.18 Å), respectively. *2B2* ($E = -234312$ kcal/mol) corresponds to the side-chain optimization calculation of model $Iso^{-}.NADP^{+}.Lys66^{+}$.Glu201.Cys58.Cys63.GSSG case 2 (initial distance between Iso atom N_5 and amine 66 atom N_z set at 2.58 Å). *Numbers* near each group or atom correspond to effective charge values. "∼" and "*" as in Fig. 2

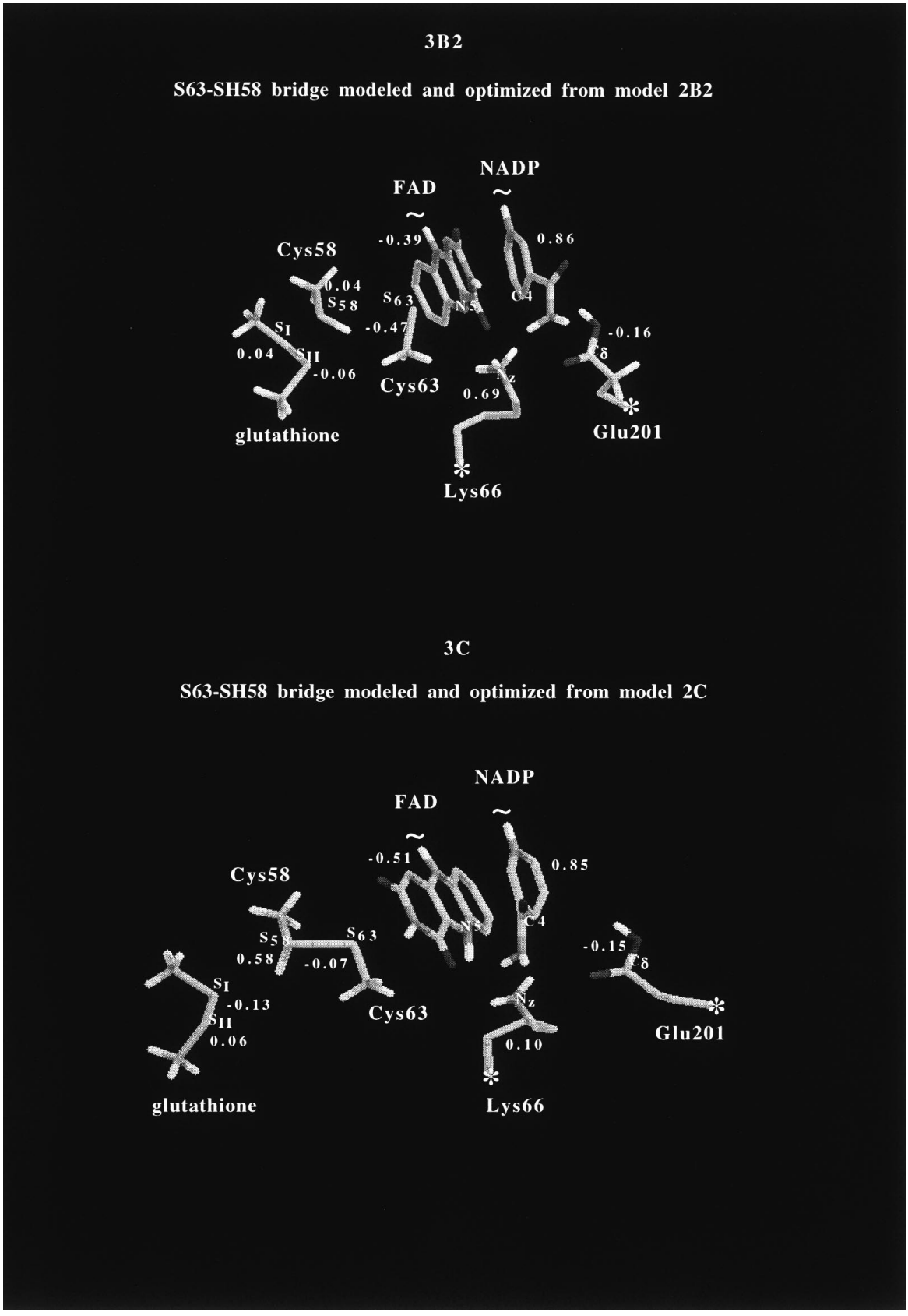

Fig. 4. G-site expanded models. *3B2* ($E = -234455$ kcal/mol) is Cys58 and Cys63 sulfur optimization calculation of model Iso^{-}.$NADP^{+}$.$Lys66^{+}$.Glu201.CysH58.Cys63.GSSG, final distance between S_{58} and S_{63} of 4.0 Å. *3C* ($E = -234474$ kcal/mol) is Cys58 and Cys63 sulfur optimization calculation of model $IsoH^{-}$.$NADP^{+}$.Lys66.Glu201.CysH58.Cys63.GSSG, final distance between S_{58} and S_{63} of 2.3 Å. *Numbers* near each group or atom correspond to effective charge values. "∼" and "*" as in Fig. 2

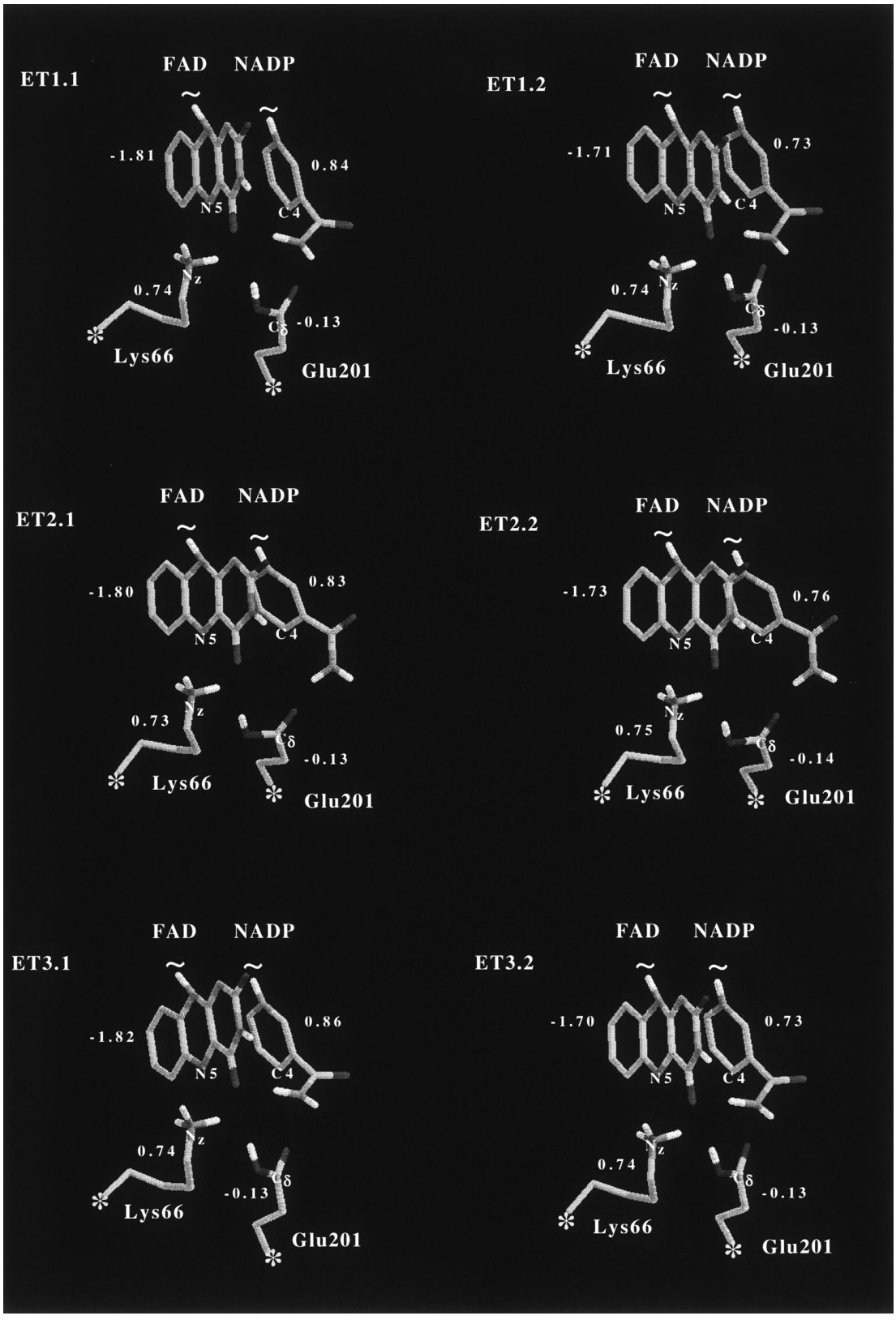

Fig. 5. Electron-transfer models. *ET1.1* and *ET1.2* with N_5 acceptor and nicotinamide C_4 donor set initially at 3.0 Å; *ET2.1* and *ET2.2*, same distance set at 3.4 Å; *ET3.1* and *ET3.2*, same distance set at 3.5 Å. The structures *ETx.1* correspond to full optimization of the Iso and NADP rings. Those labelled as *ETx.2* account for full optimization of the Iso ring and optimization of the nicotinamide ring fixing its point of linkage with the rest of the NADP molecule. *Numbers* near each group or atom correspond to effective charge values. "∼" and "*" as in Fig. 2

mol) by roughly 30 kcal/mol. The ET structure is below the TS energy, however. One factor contributing to the energy difference is the protonation state of the Lys66–Glu201 system.

4 Discussion

We have considered and evaluated the possible role of two protein residues, Lys66 and Glu201, in the formation of different complexes related to SO and ping-pong mechanisms. Binary and tertiary complexes were characterized in agreement with the SO mechanism. Besides these structures, a binary FAD–NADP model complex was found showing a fully fledged ET configuration. This latter configuration corresponds to the stage before the oxidized coenzyme leaves the N-site in the standard ping-pong mechanism. In both cases, the role of Lys66 and Glu201 was shown to be essential. All these complexes are related to the HT step since to form the ET configuration the hydride at C_4 in NADPH must have been transferred.

From the experimental viewpoint, the stereoselectivity at C_4 in NADPH indicates that the hydrogen exchanged corresponds to the one facing the FAD ring [9–12]. The theoretical results presented here agree with this constraint. The model used suggests that if HT is the common step, the stereochemical requirement is fulfilled in both cases.

The energetics of this model have to be measured from the TS. Once the pathway to the successor complex states via HT is taken and depending upon acid–base equilibria at the N-site involving Lys66–Glu201, either ET or charge-transfer structures become available. In this respect, one can look at the actual values of the TS and precursor complex. The TS with equivalent side-chain arrangements lies at 4 kcal/mol above (the not fully optimized) 1A2, and for the arrangement characteristic of 1C it is 8 kcal/mol above it. Complementary information concerning the reaction pathway is provided by the complex where the hydrogen is still at the C_4 position in the nicotinamide ring (precursor complex). With only side chains optimized as for 1A2, the activation energy is about 9 kcal/mol. As the ET structure requires the previous deprotonation of C_4, these species are to be found once the TS is formed. The calculations, including polarization (which does not change the overall trend), suggest that the redox process may go via a unique HT TS.

The choice of mechanism depends upon the binding–unbinding mechanism of $NADP^+$. This is a complex process [30], and in GR is clear that it controls the fate of the mechanism [3, 4]. The mutation Tyr177Gly leading to a SO mechanism may affect the unbinding $NADP^+$ mechanism; however, in trypanothione reductase (TR), a closely related enzyme that has glycine at the position equivalent to Tyr177 in GR, there is a ping-pong mechanism under physiological conditions [31]. If a mechanical application of the explanation for GR were made, the trypanothione reductase would have had a SO mechanism. Although one may argue that the numerous differences in sequence and small structural differences between GR and TR would compensate for the point mutation in GR, leading to rapid $NADP^+$ unbinding compared to the trypanothione binding. One can sense the complexity of the real situation. Although the present calculations are too elementary to give a definite answer to this query, it is apparent that ET occurs if the ring distance relaxes towards large values faster than substrate binding at the G-site.

To conclude, if the hypothesis of a common HT TS turned out to be correct, the variety of mechanisms in GR and possibly TR, observed under different experimental circumstances, would be due to different interactions between protein–coenzyme and/or protein primary sequence. A common HT step would join the opinion, proposed by Mattevi et al. [32], that this type of mechanism in flavoenzyme catalysis is a common fea-

Table 4. AM1 energies and effective charges for the fully optimized binary models representing hydride and electron transfer cases. *a*: full optimization of Iso and nicotinamide rings; *b*: full optimization of the Iso ring and optimization of nicotinamide ring fixing its point of linkage with the rest of the NADP molecule. *ETx.1*: full optimization of the Iso and nicotinamide rings. *ETx.2*: full optimization of the Iso ring and optimization of the nicotinamide ring fixing its point of linkage with the rest of the NADP molecule

Models	Group charges				$-E$ (kcal/mol)
	Isoalloxazine	Nicotinamide	Amine66	Carboxylate201	
1A2					
a	−0.98	0.98	0.70	−0.88	200777
b	−0.99	0.98	0.70	−0.88	200774
1C					
a	−0.99	0.99	−0.09	−0.11	200779
b	−0.99	0.98	−0.09	−0.11	200774
ET1.1	−1.81	0.84	0.74	−0.13	200744
ET1.2	−1.71	0.73	0.74	−0.13	200742
ET2.1	−1.80	0.83	0.75	−0.13	200739
ET2.2	−1.73	0.76	0.75	−0.14	200738
ET3.1	−1.82	0.86	0.74	−0.13	200744
ET3.2	−1.70	0.73	0.74	−0.13	200742

ture. A corollary concerns the ET mechanism in GR, which would actually require of a TS to be accomplished. This idea agrees with recent proposals made by Formosinho et al. [33] to describe ET reactions in solution.

Acknowledgements. The authors thank the SAREC/SIDA program for sustaining the activities in Uruguay. O.T. thanks the Swedish Research Council for continued financial support.

References

1. Pai E, Schulz GE (1983) J Biol Chem 258: 1752
2. Massey V, Williams CH (1982) Flavins and flavoproteins Elsevier-North Holland, New York
3. Mannervik B (1973) Biochem Biophys Res Commum 53: 1153
4. Williams CH (1976) In: Boyer PD (ed) The enzymes. Academic Press, New York, p 89
5. Berry A, Scrutton NS, Perham RN (1989) Biochemistry 28: 1264
6. Diaz W, Aullo JM, Paulino M, Tapia O (1996) Chem Phy 204: 195
7. Karplus PA, Schulz GE (1989) J Mol Biol 210: 163
8. Horjales E, Oliva B, Stamato FMLG, Paulino-Blumenfeld M, Nilsson O, Tapia O (1992) Mol Eng 1: 357
9. Stern BK, Vennesland B (1960) J Biol Chem 235: 209
10. Ghisla S, Massey V (1986) Biochem J 239: 1
11. Ghisla S, Massey V (1989) Eur J Biochem 181: 1
12. Manstein DJ, Pai EF, Schopfer LM, Massey V (1986) Biochemistry 25: 6807
13. Dewar DMJS, Zoebish EGG, Healy EF, Stewart JJP (1985) J Am Chem Soc 107: 3902
14. Fairlamb AH, Blackburn P, Ulrich P, Chait BT, Cerami A (1985) Science 227: 1485
15. Karplus PA, Pai EF, Schulz GE (1989) Eur J Biochem 178: 693
16. Schirmer RH, Müller JG, Krauth-Siegel RL (1995) Angew Chem Int Ed Engl 34: 141
17. Mannervik B (1976) In: Singer TP (ed) Flavins and flavoproteins. Elsevier, Amsterdam, p 485
18. Mannervik B, Boggaram V, Carlberg I (1982) In: Massey V, Williams CH (eds) Flavins and flavoproteins. Elsevier, Amsterdam, p 145
19. Mannervik B (1975) Biosystems 7: 101
20. Carlberg I, Mannervik B (1986) J Biol Chem 261: 1629
21. Pai E (1991) Curr Opin Struct Biol 1: 796
22. Karplus PA, Schulz GE (1987) J Mol Biol 195: 701
23. Cramer CJ, Truhlar DG (1992) Science 256: 213
24. Cambillau CC, Horjales E (1987) J Mol Graph 5: 174
25. Nilsson O (1990) J Mol Graph 8: 192
26. Stewart JJP (1989) J Comput Chem 10: 209
27. Tapia O, Andres J, Safont VS (1994) J Phys Chem 98: 4821
28. Zheng Y-J, Bruice TC (1997) J Am Chem Soc 119: 8137
29. Moliner V, Andrés J, Oliva M, Safont VS, Tapia O (1998) Theor Chem Acc 101: 228
30. (a) Adolph HW, Kiefer M, Cedergren-Zeppezauer E (1997) Biochemistry 36: 8743; (b) Scrutton NS, Berry A, Perham RN (1990) Nature 343: 38
31. Borges A, Cunningham ML, Fairlamb AH (1995) Eur J Biochem 228
32. Mattevi A, Vanoni MA, Curti B (1997) Curr Opin Struct Biol 7: 804
33. Formosinho SJ, Arnaut LG, Fausto R (1998) Prog React Kinet 23: 1